

A numerical method to model dynamic behavior of thin inextensible elastic rods in three dimensions

Stephen Montgomery-Smith

Department of Mathematics
University of Missouri
Columbia MO 65211
stephen@missouri.edu

Weijun Huang

Mechanical and Aerospace Engineering
University of Missouri
Columbia MO 65211
whfy6@mail.missouri.edu

ABSTRACT

Static equations for thin inextensible elastic rods, or elastica as they are sometimes called, have been studied since before the time of Euler. In this paper, we examine how to model the dynamic behavior of elastica. We present a fairly high speed, robust numerical scheme that uses (i) a space discretization that uses cubic splines, and (ii) a time discretization that preserves a discrete version of the Hamiltonian. A good choice of numerical scheme is important, because these equations are very stiff, that is, most explicit numerical schemes will become unstable very quickly. The authors conducted this research anticipating describing the dynamic Kirchhoff problem, that is, the behavior of general springs that have natural curvature, and for which the equations take into account torsion of the rod.

1 Introduction

The purpose of this research is to find an efficient and robust numerical scheme that simulates the dynamic behavior of springs, including springs that are not necessarily helical. For our purposes, we will define a spring to be a rod made out of an infinitesimally thin piece of wire, which has a natural curvature, is inextensible, and thereafter acts in an elastic fashion, possibly with damping, but with no plasticity. The general theory of elastic rods is referred to as the Kirchhoff problem, and is described in the classic work of Love [20].

In this paper, we make a modest beginning by modeling the dynamics of *elastica*. By this we mean a spring with no natural curvature, and in which we do not consider the effect of torsion. We also assume that the properties of the wire are uniform along the length of the wire. In [22], we plan to discuss the general shaped spring.

The literature on steady state solutions for elastica is huge, and we refer the reader to Levian [18] and Love [20]. For modeling dynamic behavior, Falk and Xu [10] found a stable second order scheme for elastica, and the numerical scheme presented in their paper has many similarities to this present work. Other works on elastica include Cafilisch and Maddocks [5], Coleman and Dill [7], Dichmann, Maddocks and Pego [8], Ito [15, 16], and Maddocks and Dichmann [21].

The more general theory of springs seems to go back to the classical work of Thomson [35]. This theory established geometric relationships between the various spring parameters, such as pitch angle, static load, coil curvature, and the radius of the spring helix. However Thomson assumed that the spring is helical with constant pitch and spring radius. A later paper by Lin and Pisano [19] deals with more general helical springs, allowing the pitch angle and spring radius to vary as a function of arclength.

A very general and impressive framework is given by Pai [24, 25], in which he models highly flexible structures using finite element analysis. From a numerical point of view, he can recreate our results by setting the extensibility of the rod to a

very low value. However since our paper restricts itself to rod like structures, we believe that we can obtain faster and more robust results.

From reading various conference abstracts, we see that many people are working on solving these kinds of problems. It has been hard for us to survey the complete literature, and so there may be important works that we have missed. We mention the book by Antman [1] which gives a mathematically rigorous account, the Ph.D. thesis of Goss [12] which described experimental results, and the web page of his adviser van der Heijden [36] which includes many applications of the study of slender rods.

Most work on elastica is in two dimensions, and since torsion is not taken into account, this is natural. However since we are anticipating including torsion in later works, we preferred to work in three dimensions. We have to make use of a Lagrange multiplier arising from keeping the arclength of the rod constant. This Lagrange multiplier has an interesting property in that it satisfies a one-dimensional Sturm-Liouville equation. This equation also appears in the theory of whips and chains by Preston [26, 27] and Thess et al [34].

2 Lagrangians, Hamiltonians, and energy conserving numerical methods

The time discretization method we present in this paper is designed to preserve the energy of the system. Many papers on energy conserving methods for Hamiltonian equations have been written, and some of these works are very deep and difficult [3, 6, 11, 17, 23, 28–33]. Many of them explicitly deal with the problems we are attempting in this paper.

We believe our approach is simpler for the following reason. Historically, the notion of representing equations of motion by Hamiltonians came after it was realized that many equations of motion came from a principle of least action. Let us consider the simple case when the kinetic energy is a simple quadratic

$$\mathcal{E} = \mathcal{E}(\mathbf{v}) = \frac{1}{2}m|\mathbf{v}|^2 \quad (1)$$

where $\mathbf{v} = \dot{\mathbf{x}}$ is the velocity in some m -dimensional space, and the potential energy $\mathcal{V} = \mathcal{V}(\mathbf{x})$ depends only upon the position \mathbf{x} . Suppose furthermore that the particle is constrained to stay in a submanifold of m -dimensional space given by the M constraints

$$C_k(\mathbf{x}) = 0 \quad 1 \leq k \leq M \quad (2)$$

The Hamiltonian approach is to introduce the *momentum* $\mathbf{p} = m\mathbf{v}$, the Hamiltonian $H = \mathcal{E}(\mathbf{p}/m) + \mathcal{V}(\mathbf{x})$, and write down the usual Hamiltonian equations of motion, and see that the Hamiltonian is conserved as the equations of motion evolve. However, prior researchers, have found it to be a struggle (albeit they have been successful in many cases) to find effective time discretizing numerical schemes that preserve the Hamiltonian.

The method presented in this paper is to go back to the Lagrangian equations from which the Hamiltonian equations were historically derived. This method of creating the equations of motion is often called Hamilton's principle. That is, we create the action

$$\mathcal{S}(\mathbf{x}) = \int_{t_1}^{t_2} (-\mathcal{E} + \mathcal{V} + C) dt \quad (3)$$

where

$$C = \sum_{k=1}^M \alpha_k C_k(\mathbf{x}) \quad (4)$$

is the term involving the Lagrange multipliers, α_k . Then Hamilton's principle (also called the principle of least action) is that the equation of motion can be found by calculating the stationary point of the action. That is, find the vector \mathbf{x} , satisfying the constraints, such that for any infinitesimal perturbation $\delta\mathbf{x}$ of \mathbf{x} , we have

$$\delta\mathcal{S}(\mathbf{x}) = \mathcal{S}(\mathbf{x} + \delta\mathbf{x}) - \mathcal{S}(\mathbf{x}) = O(|\delta\mathbf{x}|^2) \quad (5)$$

Then it is well known that the resulting equation of motions conserve the Hamiltonian

$$H(t) = \mathcal{E}(\dot{\mathbf{x}}) + \mathcal{V}(\mathbf{x}) \quad (6)$$

One of the goals of this paper is to present a time discretization numerical method that computes $\mathbf{x}_n = \mathbf{x}(t)$ for $t = nh$, and such that the following *discretized Hamiltonian* is conserved

$$H_n = \mathcal{E} \left(\frac{\mathbf{x}_{n+1} - \mathbf{x}_n}{h} \right) + \frac{\mathcal{V}(\mathbf{x}_n) + \mathcal{V}(\mathbf{x}_{n+1})}{2} \quad (7)$$

Such a scheme which preserves this discretized Hamiltonian was already presented in [10], and the philosophy behind their scheme is the same as ours. Their method works in the special case that $\mathcal{V}(\mathbf{x}) = \sum_{j=1}^m V(x_j)$. Our method works in the special case that $\mathcal{V}(\mathbf{x})$ and $C_k(\mathbf{x})$ are quadratic functions of \mathbf{x} . In future papers (for example, where we solve the more general spring problem), we will present numerical methods that conserve the discretized Hamiltonian in a wider class of circumstances.

The paper by Simo, Tarmow and Wong [32] discusses the case when the kinetic and potential energies are quadratic functions. But as they point out, this only gives linear dynamics. But it turns out that adding quadratic constraints give extremely interesting non-linear dynamics. For example, the work on rigid motions by Simo and Wong [30] could have been done using quadratic constraints (since the condition that a matrix is orthogonal is a quadratic constraint on the matrix entries).

We believe that this more simple minded approach may have been missed by many researchers because in the context of Hamiltonians, the position and momentum are considered to be two different, more or less interchangeable, variables, whereas in our Lagrangian approach to the discretized Hamiltonian, position and velocity clearly play very distinct roles.

3 The Mathematical Model

We describe the path of the spring by a function $\mathbf{x} : [0, L] \rightarrow \mathbb{R}^3$

$$\mathbf{x}(s) = [x_1(s), x_2(s), x_3(s)]^T \quad (8)$$

Here s is the arclength along the rod, and hence the function $\mathbf{x}(s)$ necessarily satisfies the constraint equation

$$|\mathbf{x}'(s)|^2 = x_1'(s)^2 + x_2'(s)^2 + x_3'(s)^2 = 1 \quad (9)$$

Here the prime represents differentiation with respect to the arclength. We will represent the derivative with respect to time by placing a dot over the variable.

We assume that the material from which the rod is constructed has two parameters: ρ which is the mass per unit length of the rod, and ε which is the elasticity of the material from which the rod is made. In this paper, these will both be constant throughout the length of the rod, however removing these assumptions would not greatly complicate the exposition.

The energy of the rod consists of two parts, its kinetic energy \mathcal{E} , and its potential energy \mathcal{V} , where

$$\mathcal{E} = \int_0^L \frac{1}{2} \rho |\dot{\mathbf{x}}(s)|^2 ds \quad (10)$$

$$\mathcal{V} = \int_0^L \frac{1}{2} \varepsilon |\mathbf{x}''(s)|^2 ds \quad (11)$$

There is also a possible additional term to the kinetic energy

$$\int_0^L \frac{1}{2} \sigma |\mathbf{x}'(s)|^2 ds \quad (12)$$

where σ is the moment of inertia of the cross section perpendicular to the rod per unit length. Since we assume that the rod is infinitesimal in thickness, we will set $\sigma = 0$. However this term is non-zero in the two dimensional equations obtained by Caffisch and Maddocks [5], and used by Falk and Xu [10]. Setting $\sigma > 0$ would not add any complications.

The constraint is given by

$$C = \frac{1}{2} \int_0^L \alpha(s) |\mathbf{x}'(s)|^2 ds \quad (13)$$

where $\alpha(s)$ is the Lagrange multiplier.

We allow three different boundary conditions for each end:

$$\mathbf{x}(0) \text{ and } \mathbf{x}'(0) \text{ are known functions of } t; \text{ or} \quad (14)$$

$$\mathbf{x}(0) \text{ is a known function of } t, \text{ and} \quad (15)$$

$$\mathbf{x}'(0) \text{ is not a known function of } t; \text{ or} \quad (16)$$

$$\text{neither } \mathbf{x}(0) \text{ nor } \mathbf{x}'(0) \text{ are known functions of } t. \quad (16)$$

and

$$\mathbf{x}(L) \text{ and } \mathbf{x}'(L) \text{ are known functions of } t; \text{ or} \quad (17)$$

$$\mathbf{x}(L) \text{ is a known function of } t, \text{ and} \quad (18)$$

$$\mathbf{x}'(L) \text{ is not a known function of } t; \text{ or} \quad (18)$$

$$\text{neither } \mathbf{x}(L) \text{ nor } \mathbf{x}'(L) \text{ are known functions of } t. \quad (19)$$

When we apply Hamilton's method, we suppose in the case that any of the conditions (14), (15), (17) or (18) are satisfied, that the known functions of t are constant. However once the solution to equation (5) is found, the solution is still valid in the case that the known functions of t are not constant.

Theorem 1. *The variation equation $\delta S = 0$ is solved by the equations*

$$\rho \ddot{\mathbf{x}} + \epsilon \mathbf{x}'''' - (\alpha \mathbf{x}')' = 0 \quad (20)$$

with additional boundary conditions

$$\mathbf{x}''(0) = 0 \text{ if (15);} \quad (21)$$

$$\mathbf{x}''(0) = \mathbf{x}'''(0) = 0 \text{ if (16);} \quad (22)$$

$$\mathbf{x}''(L) = 0 \text{ if (18);} \quad (23)$$

$$\mathbf{x}''(L) = \mathbf{x}'''(L) = 0 \text{ if (19).} \quad (24)$$

It can be shown that α satisfies

$$\alpha'' - |\mathbf{x}''|^2 \alpha = -\rho |\dot{\mathbf{x}}'|^2 - \epsilon (4\mathbf{x}'''' \cdot \mathbf{x}'' + 3|\mathbf{x}'''|^2) \quad (25)$$

with boundary conditions

$$\alpha'(0) = \rho \dot{\mathbf{x}}(0) \cdot \mathbf{x}'(0) - 3\epsilon \mathbf{x}''(0) \cdot \mathbf{x}'''(0) \text{ if (14) or (15);} \quad (26)$$

$$\alpha(0) = 0 \text{ if (16);} \quad (27)$$

$$\alpha'(L) = \rho \dot{\mathbf{x}}(L) \cdot \mathbf{x}'(L) - 3\epsilon \mathbf{x}''(L) \cdot \mathbf{x}'''(L) \text{ if (17) or (18);} \quad (28)$$

$$\alpha(L) = 0 \text{ if (19).} \quad (29)$$

Note that the equation for α will have a unique solution if and only if the Sturm-Liouville operator

$$-\beta'' + |\mathbf{x}''|^2 \beta \quad (30)$$

$$\beta'(0) = \beta'(L) = 0 \text{ if ((14) or (15)) and ((17) or (18))}$$

$$\beta(0) = \beta'(L) = 0 \text{ if (16) and ((17) or (18))} \quad (31)$$

$$\beta'(0) = \beta(L) = 0 \text{ if ((14) or (15)) and (19)}$$

$$\beta(0) = \beta(L) = 0 \text{ if (16) and (19)}$$

doesn't have zero in its spectrum. This will be the case whenever condition (16) or (19) hold, or whenever the rod isn't a straight line (that is \mathbf{x}'' is not identically zero), because in these circumstances the Sturm-Liouville operator is positive definite. See [2, 9].

For example, to see that α is unique when $\mathbf{x}(0)$ and $\mathbf{x}(L)$ are known functions of t and the rod isn't a straight line, suppose that α_1 and α_2 are solutions. Then $\beta = \alpha_1 - \alpha_2$ satisfies

$$-\beta'' + |\mathbf{x}''|^2\beta = 0, \quad \beta'(0) = \beta'(L) = 0 \quad (32)$$

and hence integrating by parts we see

$$\int_0^L |\beta'|^2 + |\mathbf{x}''\beta|^2 ds = \int_0^L \beta(-\beta'' + |\mathbf{x}''|^2\beta) ds = 0 \quad (33)$$

We have that $\beta' = 0$, and hence β is constant. But also $\mathbf{x}''\beta = 0$, and hence if $\mathbf{x}''(s) \neq 0$ for some s , then $\beta = 0$.

Note that if $\mathbf{x}(0)$ and $\mathbf{x}(L)$ are known functions of t , then it is physically reasonable that equation (25) with the boundary conditions may not have a unique solution if the rod isn't straight, because it is possible that the rod is being pulled apart.

Proof of Theorem 1. The variation of the action with respect to \mathbf{x} is

$$\begin{aligned} & \int_{t=t_0}^{t_1} \int_{s=0}^L -\rho \delta \dot{\mathbf{x}} \cdot \dot{\mathbf{x}} + \varepsilon \delta \mathbf{x}'' \cdot \mathbf{x}'' + \alpha \delta \mathbf{x}' \cdot \mathbf{x}' ds dt \\ &= \int_{t=t_0}^{t_1} [\varepsilon \delta \mathbf{x}' \cdot \mathbf{x}'']_{s=0}^L - [\delta \mathbf{x} \cdot (\varepsilon \mathbf{x}''' - \alpha \mathbf{x}')]_{s=0}^L \\ & \quad + \int_{s=0}^L \delta \mathbf{x} \cdot (\rho \ddot{\mathbf{x}} + \varepsilon \mathbf{x}'''' - (\alpha \mathbf{x}')') ds dt \end{aligned} \quad (34)$$

Setting the variation equal to zero, since $\delta \mathbf{x}$ is an arbitrary function of t with the exception that it must be zero at $t = t_0$ or $t = t_1$, we obtain

$$\begin{aligned} & [\varepsilon \delta \mathbf{x}' \cdot \mathbf{x}'']_{s=0}^L - [\delta \mathbf{x} \cdot (\varepsilon \mathbf{x}''' - \alpha \mathbf{x}')]_{s=0}^L \\ & + \int_{s=0}^L \delta \mathbf{x} \cdot (\rho \ddot{\mathbf{x}} + \varepsilon \mathbf{x}'''' - (\alpha \mathbf{x}')') ds = 0 \end{aligned} \quad (35)$$

We obtain equation (20) because $\delta \mathbf{x}(s)$ is arbitrary on any closed subinterval of $(0, L)$.

Next, since

$$|\mathbf{x}'|^2 = 1 \quad (36)$$

differentiating up to four times with respect to s , we obtain

$$\mathbf{x}' \cdot \mathbf{x}'' = 0 \quad (37)$$

$$|\mathbf{x}''|^2 = -\mathbf{x}' \cdot \mathbf{x}''' \quad (38)$$

$$\mathbf{x}' \cdot \mathbf{x}'''' = -3\mathbf{x}'' \cdot \mathbf{x}''' \quad (39)$$

$$\mathbf{x}'''' \cdot \mathbf{x}' = -4\mathbf{x}'''' \cdot \mathbf{x}'' - 3|\mathbf{x}''|^2 \quad (40)$$

and differentiating twice with respect to t , we obtain

$$\ddot{\mathbf{x}}' \cdot \mathbf{x}' = -|\dot{\mathbf{x}}'|^2 \quad (41)$$

Differentiating equation (20) with respect to s , we obtain

$$\rho \ddot{\mathbf{x}}' + \varepsilon \mathbf{x}'''' - \alpha'' \mathbf{x}' - 2\alpha' \mathbf{x}'' - \alpha \mathbf{x}''' = 0 \quad (42)$$

and dot producting both sides with \mathbf{x}' we obtain equation (25).

Now let us show the boundary conditions for $s = 0$, the boundary conditions for $s = L$ following by the same argument. First, dot producting equation (20) by \mathbf{x}' gives (26). Next, if condition (15) holds, then since $\delta\mathbf{x}(0)$ is arbitrary, it follows that $\mathbf{x}''(0) = 0$.

If condition (16) holds, then both $\delta\mathbf{x}(0)$ and $\delta\mathbf{x}'(0)$ are arbitrary, and hence

$$\mathbf{x}''(0) = 0 \quad (43)$$

$$\boldsymbol{\varepsilon}\mathbf{x}'''(0) - \boldsymbol{\alpha}(0)\mathbf{x}'(0) = 0 \quad (44)$$

Dot producting (44) by $\mathbf{x}'(0)$, we obtain

$$\alpha(0) = \boldsymbol{\varepsilon}\mathbf{x}'(0) \cdot \mathbf{x}'''(0) = -\boldsymbol{\varepsilon}|\mathbf{x}''(0)|^2 = 0 \quad (45)$$

Substituting back into (44) gives $\mathbf{x}'''(0) = 0$, and hence we obtain (22) and (27).

4 The Hamiltonian and Damping Terms

We define the Hamiltonian to be

$$H = \int_0^L \frac{1}{2}\rho|\dot{\mathbf{x}}|^2 + \frac{1}{2}\boldsymbol{\varepsilon}|\mathbf{x}''|^2 ds \quad (46)$$

It is well known that the Hamiltonian is a conserved quantity of the equations of motion. However we will include a detailed statement and short proof. This will help us to understand what terms we might like to use as the damping terms.

The authors do not know any general theory of how to generate the damping terms. Our idea is to find terms that will cause the Hamiltonian to be a non-increasing function of time, and such that the energy lost in the Hamiltonian could reasonably be ascribed to creating thermal energy.

Theorem 2. *Suppose that \mathbf{x} satisfies the variation of the action S is zero along with equation (9). Suppose further that in the case that any of the conditions (14), (15), (17) or (18) are satisfied that the known functions of t are constant. Then the Hamiltonian is conserved, that is*

$$\dot{H} = 0 \quad (47)$$

Proof. Dot product both sides of equation (20) with $\dot{\mathbf{x}}$, and integrate with respect to s from 0 to L , to obtain

$$\begin{aligned} 0 &= \int_0^L \dot{\mathbf{x}} \cdot (\rho\ddot{\mathbf{x}} + \boldsymbol{\varepsilon}\mathbf{x}'''' - (\boldsymbol{\alpha}\mathbf{x}')') ds \\ &= [\boldsymbol{\varepsilon}\dot{\mathbf{x}} \cdot \mathbf{x}''']_0^L - [\boldsymbol{\varepsilon}\dot{\mathbf{x}}' \cdot \mathbf{x}''']_0^L + [\boldsymbol{\alpha}\dot{\mathbf{x}}' \cdot \dot{\mathbf{x}}]_0^L \\ &\quad + \int_0^L \rho\dot{\mathbf{x}} \cdot \ddot{\mathbf{x}} + \boldsymbol{\varepsilon}\dot{\mathbf{x}}' \cdot \mathbf{x}'' + \boldsymbol{\alpha}\dot{\mathbf{x}}' \cdot \mathbf{x}' ds \\ &= [\boldsymbol{\varepsilon}\dot{\mathbf{x}} \cdot \mathbf{x}''']_0^L - [\boldsymbol{\varepsilon}\dot{\mathbf{x}}' \cdot \mathbf{x}''']_0^L + [\boldsymbol{\alpha}\dot{\mathbf{x}}' \cdot \dot{\mathbf{x}}]_0^L + \dot{H} \\ &\quad + \int_0^L \frac{1}{2}\boldsymbol{\alpha} \left(\frac{\partial}{\partial t} |\mathbf{x}'|^2 \right) ds \end{aligned} \quad (48)$$

It can be seen that under any of the boundary conditions the cross terms disappear, and also the last integral disappears because of equation (9).

This suggests that we could introduce damping terms with the view that the new equations should imply $\dot{H} \leq 0$ under the same hypothesis as Theorem 2. Furthermore, any damping term should be such that whenever the rod experiences some kind of internal change, energy is transformed into thermodynamic heat. An example of such an internal change is \mathbf{x}'' changing, but would not be \mathbf{x}' changing since the latter merely reflects a change of frame of reference. (But if the rod is operating in

an atmosphere that is stationary, then one might expect damping to be caused by \mathbf{x} changing. We won't consider this last possibility.)

Thus it seems reasonable that that any damped equation should imply something like

$$\dot{H} = -\nu \int_0^L |\dot{\mathbf{x}}''|^2 ds \quad (49)$$

where ν is a damping constant. By following the proof of Theorem 2, if we replace equation (20) by

$$\rho \ddot{\mathbf{x}} + \epsilon \mathbf{x}'''' - \nu \dot{\mathbf{x}}'''' - (\alpha \mathbf{x}')' = 0 \quad (50)$$

with appropriate changes to equations (25), (26) and (28), we see that equation (49) is satisfied. Thus, we propose equation (50) as the *damped* version of the dynamic equation of the elastic rod.

5 The Space Discretization

We approximate the path of the elastica by a cubic spline. We pick some positive integer N , and set the space mesh size $\eta = L/N$. We define

$$\mathbf{x}_j = \mathbf{x}(\eta j) \quad (0 \leq j \leq N) \quad (51)$$

suppose that $\mathbf{x}(s)$ is a cubic spline passing through these points, that is, $\mathbf{x}(s)$ is a piecewise cubic function for $j\eta \leq s \leq (j+1)\eta$, and it has a continuous second derivative.

In addition, if the rod satisfies boundary condition (14), we will choose a spline that is clamped at $s = 0$ satisfying the same boundary condition. Similarly for the boundary condition (17).

If the rod satisfies the boundary condition (15) or (16), then inspired by Theorem 1, the spline will be free at $s = 0$, that is, the spline will satisfy the boundary condition $\mathbf{x}''(0) = 0$. (In the case boundary condition (16) is satisfied, we might be tempted to try the additional boundary condition $\mathbf{x}'''(0) = 0$, but since it is a cubic spline it is unreasonable to expect this to be satisfied.) Again, similarly for the boundary condition (18) or (19).

We denote the first and second derivatives of the spline

$$\mathbf{x}'_j = \mathbf{x}'(\eta j), \quad \mathbf{x}''_j = \mathbf{x}''(\eta j) \quad (0 \leq j \leq N) \quad (52)$$

It is well known that these derivatives can be computed using the following matrices (see for example [4]):

$$A = \begin{bmatrix} A_{0,0} & A_{0,1} & 0 & 0 & \cdots & 0 & 0 \\ \eta & 4\eta & \eta & 0 & \cdots & 0 & 0 \\ 0 & \eta & 4\eta & \eta & \cdots & 0 & 0 \\ 0 & 0 & \eta & 4\eta & \cdots & 0 & 0 \\ \vdots & \vdots & \vdots & \vdots & \ddots & \vdots & \vdots \\ 0 & 0 & 0 & 0 & \cdots & 4\eta & \eta \\ 0 & 0 & 0 & 0 & \cdots & A_{N,N-1} & A_{N,N} \end{bmatrix} \quad (53)$$

where

$$A_{0,0} = 2\eta, A_{0,1} = \eta \text{ if condition (14) holds;} \quad (54)$$

$$A_{0,0} = 1, A_{0,1} = 0 \text{ if condition (15) or (16) hold;} \quad (55)$$

$$A_{N,N-1} = \eta, A_{N,N} = 2\eta \text{ if condition (17) holds;} \quad (56)$$

$$A_{N,N-1} = 0, A_{N,N} = 1 \text{ if condition (18) or (19) hold.} \quad (57)$$

$$\mathbf{U} = \frac{1}{\eta} \begin{bmatrix} U_{0,0} & U_{0,1} & 0 & 0 & \cdots & 0 & 0 \\ 3 & -6 & 3 & 0 & \cdots & 0 & 0 \\ 0 & 3 & -6 & 3 & \cdots & 0 & 0 \\ 0 & 0 & 3 & -6 & \cdots & 0 & 0 \\ \vdots & \vdots & \vdots & \vdots & \ddots & \vdots & \vdots \\ 0 & 0 & 0 & 0 & \cdots & -6 & 3 \\ 0 & 0 & 0 & 0 & \cdots & U_{N,N-1} & U_{N,N} \end{bmatrix} \quad (58)$$

where

$$U_{0,0} = -3, U_{0,1} = 3 \text{ if condition (14) holds;} \quad (59)$$

$$U_{0,0} = 0, U_{0,1} = 0 \text{ if condition (15) or (16) hold;} \quad (60)$$

$$U_{N,N-1} = 3, U_{N,N} = -3 \text{ if condition (17) holds;} \quad (61)$$

$$U_{N,N-1} = 0, U_{N,N} = 0 \text{ if condition (18) or (19) hold.} \quad (62)$$

$$\mathbf{B} = \frac{1}{\eta} \begin{bmatrix} -1 & 1 & 0 & 0 & \cdots & 0 & 0 \\ 0 & -1 & 1 & 0 & \cdots & 0 & 0 \\ 0 & 0 & -1 & 1 & \cdots & 0 & 0 \\ 0 & 0 & 0 & -1 & \cdots & 0 & 0 \\ \vdots & \vdots & \vdots & \vdots & \ddots & \vdots & \vdots \\ 0 & 0 & 0 & 0 & \cdots & -1 & 1 \\ 0 & 0 & 0 & 0 & \cdots & -1 & 1 \end{bmatrix} \quad (63)$$

$$\mathbf{C} = \frac{\eta}{3} \begin{bmatrix} 2 & 1 & 0 & 0 & \cdots & 0 & 0 \\ 0 & 2 & 1 & 0 & \cdots & 0 & 0 \\ 0 & 0 & 2 & 1 & \cdots & 0 & 0 \\ 0 & 0 & 0 & 2 & \cdots & 0 & 0 \\ \vdots & \vdots & \vdots & \vdots & \ddots & \vdots & \vdots \\ 0 & 0 & 0 & 0 & \cdots & 2 & 1 \\ 0 & 0 & 0 & 0 & \cdots & -1 & -2 \end{bmatrix} \quad (64)$$

From now on we employ an abuse of notation, and allow \mathbf{x} , \mathbf{x}' and \mathbf{x}'' to denote either the functions on $[0, L]$, or the vectors

$$\mathbf{x} = [\mathbf{x}_0, \mathbf{x}_1, \dots, \mathbf{x}_N]^T \quad (65)$$

$$\mathbf{x}' = [\mathbf{x}'_0, \mathbf{x}'_1, \dots, \mathbf{x}'_N]^T \quad (66)$$

$$\mathbf{x}'' = [\mathbf{x}''_0, \mathbf{x}''_1, \dots, \mathbf{x}''_N]^T \quad (67)$$

where which notation we intend should be obvious from the context. Here each of the entries of these vectors is itself a three dimensional vector¹. We also denote

$$\mathbf{z} = [\mathbf{z}_0, 0, 0, \dots, 0, \mathbf{z}_N]^T \quad (68)$$

with

$$\mathbf{z}_0 = \mathbf{x}'(0) \text{ if condition (14) holds;} \quad (69)$$

$$\mathbf{z}_0 = 0 \text{ if condition (15) or (16) hold;} \quad (70)$$

$$\mathbf{z}_N = -\mathbf{x}'(L) \text{ if condition (17) holds;} \quad (71)$$

$$\mathbf{z}_N = 0 \text{ if condition (18) or (19) hold.} \quad (72)$$

¹Some people might argue that a vector of vectors should really be called a tensor.

Then

$$\mathbf{x}'' = D_2 \mathbf{x} - 6A^{-1} \mathbf{z} \quad (73)$$

$$\mathbf{x}' = B \mathbf{x} - \frac{1}{2} C \mathbf{x}'' = D_1 \mathbf{x} + 3CA^{-1} \mathbf{z} \quad (74)$$

where

$$D_2 = 2A^{-1}U \quad (75)$$

$$D_1 = B - CA^{-1}U \quad (76)$$

Note that these matrices can be written in sparse form. In particular, A should be represented as its LU factorization, because A^{-1} is not sparse. This is because computing A^{-1} takes time $O(N^2)$ to compute, whereas $A^{-1}U\mathbf{x}$ can be computed in time $O(N)$. Similar remarks apply to $(A^T)^{-1}$.

Next, the energies and constraints are now set as

$$\mathcal{E} = \sum_{j=0}^N w_j \frac{1}{2} \rho |\dot{\mathbf{x}}_j|^2 = \frac{1}{2} \rho \boldsymbol{\eta} \dot{\mathbf{x}}^T W \dot{\mathbf{x}} \quad (77)$$

$$\begin{aligned} \mathcal{V} &= \sum_{j=0}^N w_j \frac{1}{2} \varepsilon |\mathbf{x}_j''|^2 \\ &= \frac{1}{2} \varepsilon \boldsymbol{\eta} (D_2 \mathbf{x} - 6A^{-1} \mathbf{z})^T W (D_2 \mathbf{x} - 6A^{-1} \mathbf{z}) \end{aligned} \quad (78)$$

$$\begin{aligned} \mathcal{C} &= \sum_{j=0}^N w_j \frac{1}{2} \alpha_j |\mathbf{x}'_j|^2 \\ &= \frac{1}{2} \boldsymbol{\eta} (D_1 \mathbf{x} + 3CA^{-1} \mathbf{z})^T W (\boldsymbol{\alpha} * D_1 \mathbf{x} + 3CA^{-1} \mathbf{z}) \end{aligned} \quad (79)$$

$$|\mathbf{x}'|^2 = 1 \quad (80)$$

where the Lagrange multiplier is $\boldsymbol{\alpha} = [\alpha_0, \alpha_1, \dots, \alpha_N]^T$, and the weight w_j is η unless $j = 0, N$ when it is $\frac{1}{2}\eta$, according to the trapezoidal rule for numerical integration, and W is the $(N+1) \times (N+1)$ diagonal matrix whose diagonal entries are 1 except for the top and bottom entries which are $\frac{1}{2}$, and $*$ denotes the pointwise multiplication of vectors

$$\boldsymbol{\alpha} * \mathbf{x} = [\alpha_0 \mathbf{x}_0, \alpha_1 \mathbf{x}_1, \dots, \alpha_N \mathbf{x}_N]^T \quad (81)$$

$$\mathbf{x} * \mathbf{y} = [\mathbf{x}_0 \cdot \mathbf{y}_0, \mathbf{x}_1 \cdot \mathbf{y}_1, \dots, \mathbf{x}_N \cdot \mathbf{y}_N]^T \quad (82)$$

We now apply Hamilton's principle, noting that the variation $\delta \mathbf{x}_0$ is zero if any of the conditions (14) or (15) are satisfied, and $\delta \mathbf{x}_N$ is zero if any of the conditions (17) or (18) are satisfied.

We obtain the equation

$$\begin{aligned} E \rho \ddot{\mathbf{x}} &= E W^{-1} (-\varepsilon D_2^T W D_2 \dot{\mathbf{x}} + \varepsilon 6 D_2^T W A^{-1} \mathbf{z} \\ &\quad + 3 D_1^T W (\boldsymbol{\alpha} * (CA^{-1} \mathbf{z})) + D_1^T W (\boldsymbol{\alpha} * (D_1 \dot{\mathbf{x}}))) \end{aligned} \quad (83)$$

$$(D_1 \dot{\mathbf{x}}) * (D_1 \dot{\mathbf{x}}) = 1 \quad (84)$$

Here E is the $(N+1) \times (N+1)$ diagonal matrix whose diagonal entries are 1, except for the very top and bottom entries. The top entry of E is 0 if conditions (14) or (15) hold, and 1 if (16) holds, and similarly the bottom entry of E is 0 if conditions (17) or (18) hold, and 1 if (19) holds. Thus, for example, if the top and bottom entries of E are zero, then the equation $E \mathbf{x} = E \mathbf{y}$ is really saying $\mathbf{x}_j = \mathbf{y}_j$ for $1 \leq j \leq N-1$.

For the damped equation, we present the equation

$$\begin{aligned} E \rho \ddot{\mathbf{x}} &= E W^{-1} (-\varepsilon D_2^T W D_2 \dot{\mathbf{x}} + \varepsilon 6 D_2^T W A^{-1} \mathbf{z} \\ &\quad + 3 D_1^T W (\boldsymbol{\alpha} * (CA^{-1} \mathbf{z})) + D_1^T W (\boldsymbol{\alpha} * (D_1 \dot{\mathbf{x}})) \\ &\quad + \nu D_2^T W D_2 \dot{\mathbf{x}} - \nu 6 D_2^T W A^{-1} \dot{\mathbf{z}}) \end{aligned} \quad (85)$$

6 The Time Discretization

The numerical solution to these equations turns out to be rather more difficult than simply finding some finite mesh scheme, and feeding it into ones favorite ODE solver. A big problem is that the differential equations (20), (50), (83), and (85) are examples of *stiff* equations. The notion of stiffness is well known in the theory of numerical solutions to differential equations. It happens when one part of the solution evolves far more quickly in time than another part of the solution. For example, when solving the heat equation, sharp spikes of heat will quickly dissipate, whereas broad regions of low density heat do not change much at all. The problem is that a very short time step is then needed, because otherwise the parts that decay fast will overshoot, and create large effects on the final numerical solution, whereas in actuality the eventual effect of the fast parts should be negligible. The problem of stiffness has been amply handled in the numerical differential equation literature, and today many so called ‘stiff-solvers’ are available in proprietary and open-source packages [13].

However, our equations have a different type of stiffness. Typical stiffness involves linear operators whose eigenvalues can be very large, but in the negative direction. Our equation has large eigenvalues, but in the imaginary direction. This means that instead of the fast parts quickly dissipating, they oscillate very rapidly. The problem is similar to spinning a coin, and then trying to predict the precise orientation of the coin exactly one second later. The coin will have spun many times, and the space and time measurements have to be extremely accurate.

For this reason, we take advantage of the fact that our equations come from applying Hamilton’s principle, and as explained in Section 2, we look for a method that will preserve a discretized version of the Hamiltonian.

The goal is to apply Hamilton’s principle to find the ODE which solves for the m -dimensional vector \mathbf{x} , using kinetic energy, potential energy and constraints which are of the following form:

$$\mathcal{E}(\mathbf{x}) = \frac{1}{2} \dot{\mathbf{x}}^T \mathbf{K} \dot{\mathbf{x}} \quad (86)$$

$$\mathcal{V}(\mathbf{x}) = \frac{1}{2} \mathbf{x}^T \mathbf{V} \mathbf{x} + \mathbf{v} \cdot \mathbf{x} \quad (87)$$

$$C_k(\mathbf{x}) = \frac{1}{2} \mathbf{x}^T \mathbf{C}_k \mathbf{x} + \mathbf{c}_k \cdot \mathbf{x} + \chi_k = 0 \quad 1 \leq k \leq M \quad (88)$$

$$C(\mathbf{x}) = \sum_{k=1}^M \alpha_k C_k(\mathbf{x}) \quad (89)$$

Here \mathbf{K} and \mathbf{V} are positive definite matrices, \mathbf{C}_k for $1 \leq k \leq M$ are symmetric matrices, \mathbf{c}_k for $1 \leq k \leq M$ and \mathbf{v} are vectors, and χ_k for $1 \leq k \leq M$ are scalars.

Hamilton’s principle gives the equation

$$\mathbf{K} \ddot{\mathbf{x}} = -\nabla \mathcal{V}(\mathbf{x}) - \sum_{k=1}^M \alpha_k \nabla C_k(\mathbf{x}) \quad (90)$$

and a damped version of the equation is

$$\mathbf{K} \ddot{\mathbf{x}} = -\nabla \mathcal{V}(\mathbf{x}) - \sum_{k=1}^M \alpha_k \nabla C_k(\mathbf{x}) - \mathbf{g}(\dot{\mathbf{x}}) \quad (91)$$

where

$$\mathbf{g}(\dot{\mathbf{x}}) = \mathbf{G} \dot{\mathbf{x}} \quad (92)$$

is a damping term satisfying $\dot{\mathbf{x}} \cdot \mathbf{g}(\dot{\mathbf{x}}) \geq 0$, that is, \mathbf{G} is positive semi-definite.

Now let us describe the discrete numerical scheme to solve the ODE. Pick some small time step h , and slightly abusing notation, denote \mathbf{x} at $t = nh$ by \mathbf{x}_n . The idea behind the time discretization is to find replacements for the gradients, that is, vector valued functions $\mathbf{D}\mathcal{V}(\mathbf{x}_{n-1}, \mathbf{x}_{n+1})$ and $\mathbf{D}C_k(\mathbf{x}_{n-1}, \mathbf{x}_{n+1})$ so that

$$(\mathbf{x}_{n+1} - \mathbf{x}_{n-1}) \cdot \mathbf{D}\mathcal{V}(\mathbf{x}_{n-1}, \mathbf{x}_{n+1}) = \mathcal{V}(\mathbf{x}_{n+1}) - \mathcal{V}(\mathbf{x}_{n-1}) \quad (93)$$

$$(\mathbf{x}_{n+1} - \mathbf{x}_{n-1}) \cdot \mathbf{D}C_k(\mathbf{x}_{n-1}, \mathbf{x}_{n+1}) = C_k(\mathbf{x}_{n+1}) - C_k(\mathbf{x}_{n-1}) \quad (94)$$

and

$$\mathbf{D}\mathcal{V}(\mathbf{x}_{n-1}, \mathbf{x}_{n+1}) = \nabla \mathcal{V}\left(\frac{1}{2}(\mathbf{x}_{n-1} + \mathbf{x}_{n+1})\right) + O(h^2) \quad (95)$$

$$\mathbf{D}C_k(\mathbf{x}_{n-1}, \mathbf{x}_{n+1}) = \nabla C_k\left(\frac{1}{2}(\mathbf{x}_{n-1} + \mathbf{x}_{n+1})\right) + O(h^2) \quad (96)$$

In our case, because \mathcal{V} and C_k are quadratic functions, it is easily shown that the following choices work

$$\mathbf{D}\mathcal{V}(\mathbf{x}_{n-1}, \mathbf{x}_{n+1}) = \mathbf{V}\left(\frac{1}{2}(\mathbf{x}_{n-1} + \mathbf{x}_{n+1})\right) + \mathbf{v} \quad (97)$$

$$\mathbf{D}C_k(\mathbf{x}_{n-1}, \mathbf{x}_{n+1}) = C_k\left(\frac{1}{2}(\mathbf{x}_{n-1} + \mathbf{x}_{n+1})\right) + \mathbf{c}_k \quad (98)$$

In general, the choice of $\mathbf{D}\mathcal{V}(\mathbf{x}_{n-1}, \mathbf{x}_{n+1})$ is not unique. (In the paper [10], $\mathcal{V}'(\mathbf{x})$ is of the form $\sum_{j=1}^m V(x_j)$, and so $(\mathbf{D}\mathcal{V}'(\mathbf{x}_{n-1}, \mathbf{x}_{n+1}))_j = (V(x_{n+1,j}) - V(x_{n-1,j})) / (x_{n+1,j} - x_{n-1,j})$ works.)

The discrete numerical scheme proposed is

$$\begin{aligned} \mathbf{K}\left(\frac{\mathbf{x}_{n+1} - 2\mathbf{x}_n + \mathbf{x}_{n-1}}{h^2}\right) &= -\mathbf{D}\mathcal{V}'(\mathbf{x}_{n-1}, \mathbf{x}_{n+1}) \\ &- \sum_{k=1}^M \alpha_k \mathbf{D}C_k(\mathbf{x}_{n-1}, \mathbf{x}_{n+1}) - \mathbf{g}\left(\frac{\mathbf{x}_{n+1} - \mathbf{x}_{n-1}}{2h}\right) \end{aligned} \quad (99)$$

$$C_k(\mathbf{x}_{n+1}) = 0 \quad (1 \leq k \leq M) \quad (100)$$

We assume that $C_k(\mathbf{x}_0) = C_k(\mathbf{x}_1) = 0$ ($1 \leq k \leq M$). This scheme requires solving $M + m$ non-linear equations for \mathbf{x}_{n+1} and $(\alpha_k)_{1 \leq k \leq M}$. Since the equations are quadratic, it should be easy to solve using a Newton-Raphson or a Levenberg-Marquardt algorithm, because the Jacobian is easily computed. Notice also that this scheme is of order 2 because of equations (95) and (96).

Define the *discrete Hamiltonian* by

$$H_{n+1} = \frac{1}{2h^2}(\mathbf{x}_{n+1} - \mathbf{x}_n)^T \mathbf{K}(\mathbf{x}_{n+1} - \mathbf{x}_n) + \frac{1}{2}(\mathcal{V}'(\mathbf{x}_{n+1}) + \mathcal{V}'(\mathbf{x}_n)) \quad (101)$$

Theorem 3. *The solution to difference scheme (99)-(100) satisfies that the discrete Hamiltonian is non-increasing, or constant in the case that $\mathbf{g} = 0$:*

$$H_{n+1} - H_n = -\frac{1}{2}(\mathbf{x}_{n+1} - \mathbf{x}_{n-1}) \cdot \mathbf{g}\left(\frac{1}{2h}(\mathbf{x}_{n+1} - \mathbf{x}_{n-1})\right) \leq 0 \quad (102)$$

Thus the solution to this difference scheme stays in a compact set. This guarantees that the solution will not blow up, and this suggests that the solution will be stable.

Proof. Dot product both sides of equation (99) by $\frac{1}{2}(\mathbf{x}_{n+1} - \mathbf{x}_{n-1})$. The left hand side becomes

$$\begin{aligned} &\left(\frac{\mathbf{x}_{n+1} - \mathbf{x}_{n-1}}{2}\right)^T \mathbf{K}\left(\frac{\mathbf{x}_{n+1} - 2\mathbf{x}_n + \mathbf{x}_{n-1}}{h^2}\right) \\ &= \frac{1}{2h^2}(\mathbf{x}_{n+1} - \mathbf{x}_n)^T \mathbf{K}(\mathbf{x}_{n+1} - \mathbf{x}_n) \\ &\quad - \frac{1}{2h^2}(\mathbf{x}_n - \mathbf{x}_{n-1})^T \mathbf{K}(\mathbf{x}_n - \mathbf{x}_{n-1}) \end{aligned} \quad (103)$$

The right hand side becomes

$$\begin{aligned} &-\frac{1}{2}(\mathbf{x}_{n+1} - \mathbf{x}_{n-1}) \cdot \mathbf{D}\mathcal{V}'(\mathbf{x}_{n-1}, \mathbf{x}_{n+1}) \\ &-\frac{1}{2} \sum_{k=1}^M \alpha_k (\mathbf{x}_{n+1} - \mathbf{x}_{n-1}) \cdot \mathbf{D}C_k(\mathbf{x}_{n-1}, \mathbf{x}_{n+1}) \\ &-\frac{1}{2}(\mathbf{x}_{n+1} - \mathbf{x}_{n-1}) \cdot \mathbf{g}\left(\frac{1}{2h}(\mathbf{x}_{n+1} - \mathbf{x}_{n-1})\right) \\ &= -\frac{1}{2}(\mathcal{V}'(\mathbf{x}_{n+1}) - \mathcal{V}'(\mathbf{x}_{n-1})) \\ &\quad - \frac{1}{2} \sum_{k=1}^M \alpha_k (C_k(\mathbf{x}_{n+1}) - C_k(\mathbf{x}_{n-1})) \\ &\quad - \frac{1}{2}(\mathbf{x}_{n+1} - \mathbf{x}_{n-1}) \cdot \mathbf{g}\left(\frac{1}{2h}(\mathbf{x}_{n+1} - \mathbf{x}_{n-1})\right) \\ &= -\frac{1}{2}(\mathcal{V}'(\mathbf{x}_{n+1}) + \mathcal{V}'(\mathbf{x}_n)) + \frac{1}{2}(\mathcal{V}'(\mathbf{x}_n) + \mathcal{V}'(\mathbf{x}_{n-1})) \\ &\quad - \frac{1}{2}(\mathbf{x}_{n+1} - \mathbf{x}_{n-1}) \cdot \mathbf{g}\left(\frac{1}{2h}(\mathbf{x}_{n+1} - \mathbf{x}_{n-1})\right) \end{aligned} \quad (104)$$

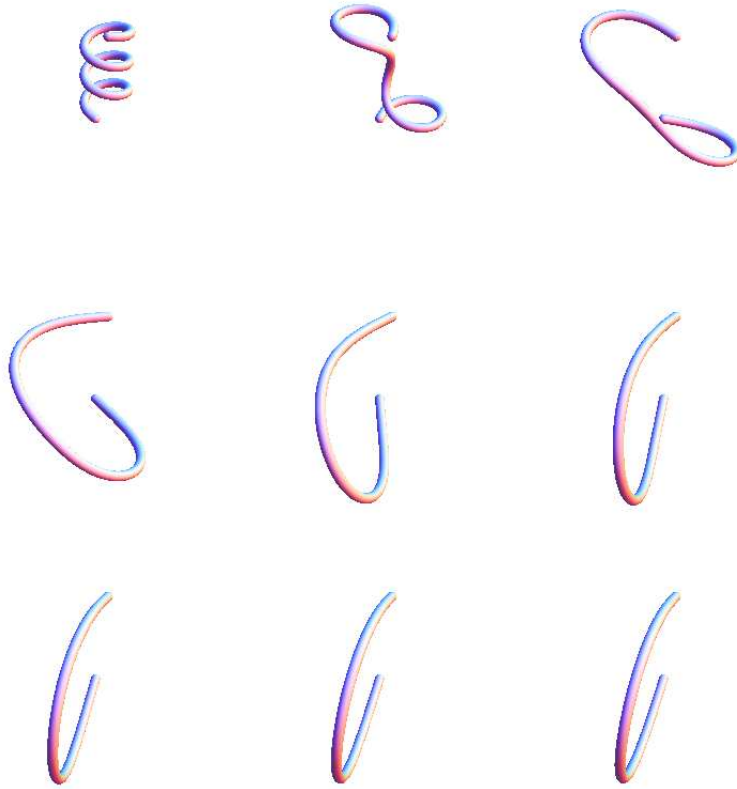


Fig. 1. A heavily damped, coiled, elastic rod unraveling.

because from equation (100) we have $C_k(\mathbf{x}_{n+1}) = C_k(\mathbf{x}_{n-1}) = 0$.

Finally, let us discuss the initial conditions. These are normally specified by assuming we know $\mathbf{x} = \mathbf{F}$ and $\dot{\mathbf{x}} = \mathbf{G}$ at $t = 0$, where \mathbf{F} and \mathbf{G} are given. To guarantee that the method is still order 2 in time, the discrete versions of these conditions are

$$\mathbf{x}_0 = \mathbf{F} \quad (105)$$

$$\mathbf{x}_1 - \mathbf{x}_{-1} = 2h\mathbf{G} \quad (106)$$

the latter equation being correct up to $O(h^3)$. Thus \mathbf{x}_0 is immediately known, and \mathbf{x}_1 can be found by substituting equation (106) into equation (99) with $n = 0$.

7 Example Implementations of the Numerical Scheme

We implemented the numerical scheme using Wolfram's *Mathematica 8* program. The first example is of an elastic rod that is initially coiled. We then let the elastic rod "unravel," assuming that both ends are fixed but allowed to rotate freely. In this case, the initial data and boundary conditions are

$$\mathbf{x}(s) = -[\sin(\sin(\theta)s), \cos(\sin(\theta)s), \cos(\theta)s]^T \quad (107)$$

$$(0 \leq s \leq L = 6\pi, \theta = 1.8, t = 0)$$

$$\dot{\mathbf{x}} = [0, 0, 0]^T \quad (t = 0) \quad (108)$$

$$\mathbf{x}(0 \text{ and } \mathbf{x}(6\pi) \text{ are fixed}) \quad (109)$$

$$\mathbf{x}'(0 \text{ and } \mathbf{x}'(6\pi) \text{ are free}) \quad (110)$$

The simulation ran with $\rho = \varepsilon = 1$, and $\nu = 10$. The program ran with $N = 50$, and a time step size of $h = 5$ with $0 \leq t \leq 100$. In Figure 1, we show the odd numbered steps up to the 17th step. The simulation took about five minutes of computer time to run on a laptop with an Intel Q740 i7 processor running at 1.73GHz.

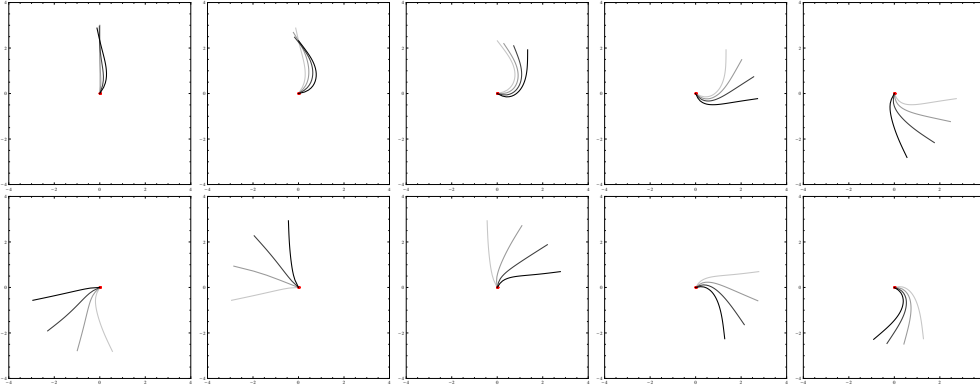


Fig. 2. An elastic rod rotating about a point.

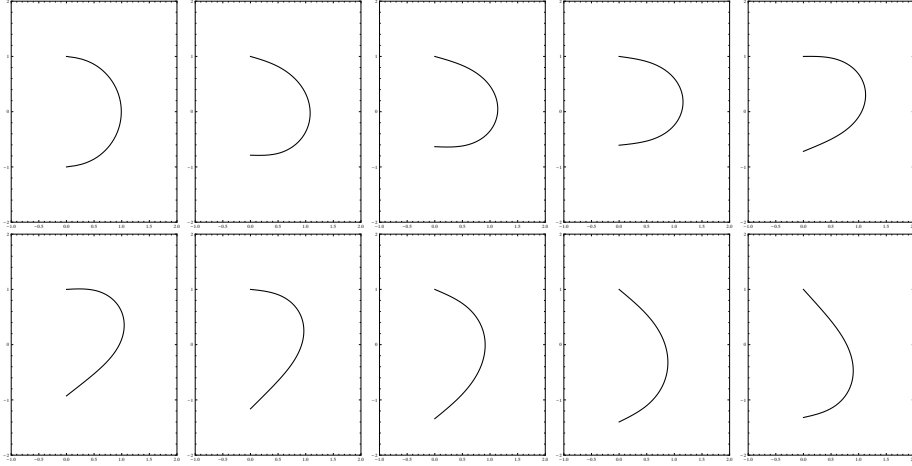


Fig. 3. An elastic rod fixed at two ends, one of which is oscillating.

The second example is an elastic rod that is initially straight. One end is free, and the other end is clamped and rotating about a single point. The initial data and boundary conditions are

$$\mathbf{x}(s) = [0, 0, s]^T \quad (0 \leq s \leq L = 3, t = 0) \quad (111)$$

$$\dot{\mathbf{x}} = [0, 0, 0]^T \quad (t = 0) \quad (112)$$

$$\mathbf{x}(0) = [0, 0, 0]^T \quad (113)$$

$$\mathbf{x}'(0) = [0, \sin(\frac{4}{5}t), \cos(\frac{4}{5}t)]^T \quad (114)$$

$$\mathbf{x}(3) \text{ and } \mathbf{x}'(3) \text{ are free} \quad (115)$$

The simulation ran with $\rho = \varepsilon = 1$, and $\nu = 1/20$. The program ran with $N = 10$, and a time step size of $h = 1/6$. In Figure 2, we show results for $0 \leq t \leq 10$. We show 60 steps, 4 steps per frame, with the first and last step of each frame matching). The simulation took about three minutes on the above described computer.

The third example is an elastic rod that is initially a semi-circle. Both ends are known functions of t , and rotate freely. One end oscillates. The intent is to show the effect of inertia on the elastic rod. The initial data and boundary conditions are

$$\mathbf{x}(s) = [\sin(s), 0, \cos(s)]^T \quad (0 \leq s \leq L = \pi, t = 0) \quad (116)$$

$$\dot{\mathbf{x}}(s) = [0, 0, 0]^T \quad (t = 0) \quad (117)$$

$$\mathbf{x}(0) = [0, 0, 1]^T \quad (118)$$

$$\mathbf{x}(\pi) = [0, 0, -1 + \frac{2}{5} \sin(2t)]^T \quad (119)$$

$$\mathbf{x}'(0) \text{ and } \mathbf{x}'(\pi) \text{ are free} \quad (120)$$

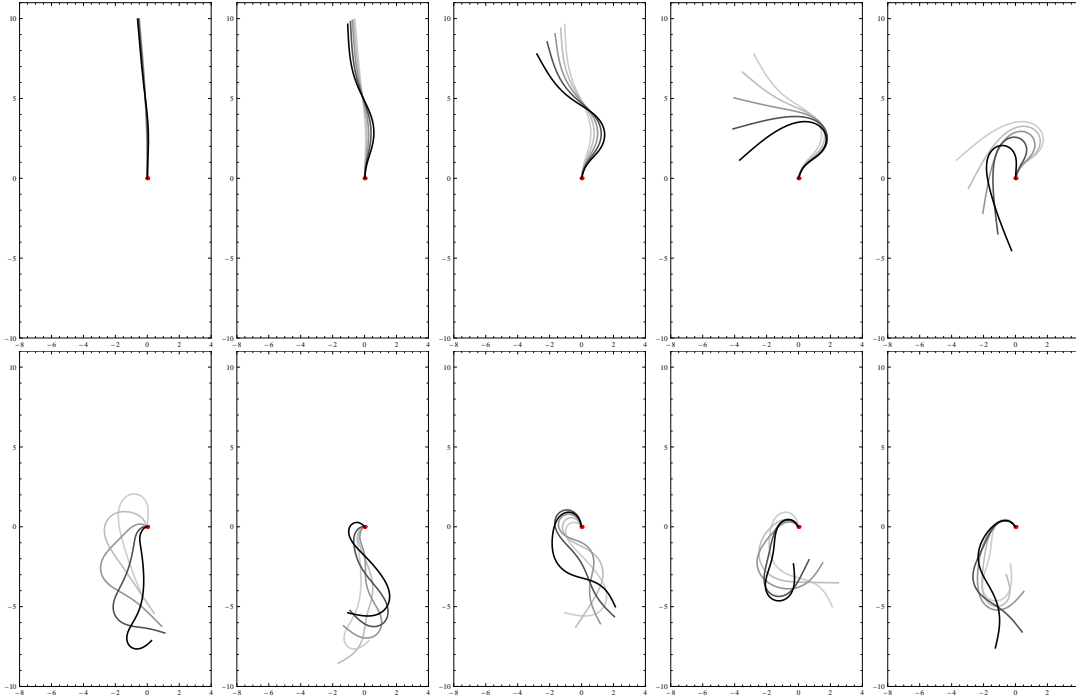


Fig. 4. An elastic rod, clamped at one end, free at the other end, under the influence of gravity.

The simulation ran with $\rho = \varepsilon = 1$, and $\nu = 1/5$. The program ran with $N = 15$, and a time step size of $h = 0.02$. In Figure 3, we show results for $0 \leq t \leq 3$. We show every 15th step up to 30 steps. The simulation took about one minute to run on the above described computer.

The final example is to simulate an elastic rod, vertical but slightly bent, clamped at the bottom and free at the top, and see how it falls under the influence of gravity. The parameters were chosen so that the fall was rather wild, to illustrate the robustness of the numerical scheme. The initial data and boundary conditions are

$$\mathbf{x}(s) = 100[\cos(s/100) - 1, 0, \sin(s/100)]^T \quad (0 \leq s \leq 10, t = 0) \quad (121)$$

$$\dot{\mathbf{x}} = [0, 0, 0]^T \quad (t = 0) \quad (122)$$

$$\mathbf{x}(0) = [0, 0, 0]^T \quad (123)$$

$$\mathbf{x}'(0) = [0, 0, 1]^T \quad (124)$$

$$\mathbf{x}(10) \text{ and } \mathbf{x}'(10) \text{ are free} \quad (125)$$

We added to the Hamiltonian a gravitational field $\mathbf{g} = [0, 0, -\frac{1}{5}]^T$ (that is, add $\rho\mathbf{g}$ to the right hand side of equation (85)), and the simulation ran with $\rho = \varepsilon = 1$, and $\nu = 0.1$. In Figure 4, we show results for $0 \leq t \leq 40$. The program ran with $N = 20$, and a time step size of $h = 0.1$, showing a total of 400 steps (5 steps per frame, with the first and last step of each frame matching). The simulation took about twenty minutes to run on the above described computer.

8 Comparison of a Numerical Solution with an Analytical Solution

Solutions to the steady state equations are well known [18,20]. For example, if a steady state elastica of length L satisfies boundary conditions (15) and (18) with

$$\mathbf{x}(0) = [-\alpha, 0, 0]^T \quad (126)$$

$$\mathbf{x}(L) = [\alpha, 0, 0]^T \quad (127)$$

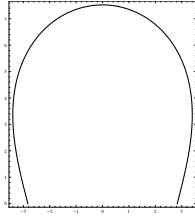


Fig. 5. A steady state solution.

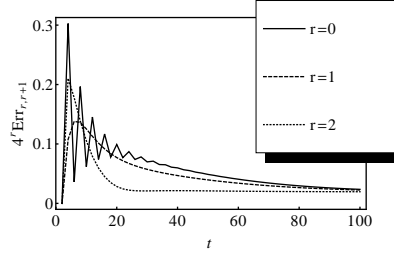


Fig. 6. Plot of $4^r \text{Err}_{r,r+1}$ for $r = 0, 1, 2$.

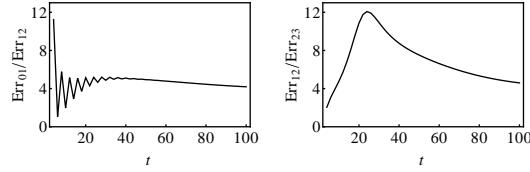


Fig. 7. Plots of $\text{Err}_{r,r+1}/\text{Err}_{r+1,r+2}$ for $r = 0, 1$.

then a solution is

$$\mathbf{x}(s) = \frac{1}{a} \begin{bmatrix} 2E(\text{am}(a(s-L/2), m), m) - a(s-L/2) \\ 2\sqrt{m} \text{cn}(a(s-L/2), m) \\ 0 \end{bmatrix} \quad (128)$$

where E is the elliptic integral of the second kind, am is the Jacobi amplitude function, and cn is the cosine Jacobi elliptic function. For example, if $L = 6\pi$ and $\alpha = 2\sqrt{2}$, then using the *Mathematica* `FindRoot` command, we find that $m = 0.624401$, $a = 0.209749$. The plot of this solution is shown in Figure 5.

We ran the numerical simulation with initial data and boundary conditions

$$\mathbf{x}(s) = [4\sin((s-3\pi)/4), 4\cos((s-3\pi)/4) + 2\sqrt{2}, 0]^T \quad (129)$$

$$(0 \leq s \leq L = 6\pi, t = 0)$$

$$\dot{\mathbf{x}} = [0, 0, 0]^T \quad (t = 0) \quad (130)$$

$$\mathbf{x}(0 \text{ and } \mathbf{x}(6\pi) \text{ are fixed}) \quad (131)$$

$$\mathbf{x}'(0 \text{ and } \mathbf{x}'(6\pi) \text{ are free}) \quad (132)$$

The simulation ran with $\rho = \varepsilon = 1$, and $\nu = 10$. The program ran with $N = 50$, and a time step size of $h = 5$ with $0 \leq t \leq 100$.

We compared the numerical solution at $t = 100$ with the analytical solution, where it is observed that the numerical solution attains a steady state. The maximum difference between the numerical solution and the analytic solution was about 0.003.

9 Numerical evidence that the numerical method is of order two

We have already indicated that the error produced by the time discretization is of order 2. It also follows from error bounds for cubic splines (see for example [14]), and error bounds for the trapezoidal rule for integration (see for example [4])

that the space discretization should also be of order 2. We have tested this numerically by performing the same computing for various values of M and N (or equivalently different values of η and h).

The example computation we chose to use was the first example in Section 7, with L changed to 2π . The computations were performed four times, with

$$(M, N) = (50 \times 2^r, 10 \times 2^r), \quad (r = 0, 1, 2, 3) \quad (133)$$

to produce solutions which we call respectively $\mathbf{x}_r(s, t)$ ($r = 0, 1, 2, 3$). We computed the root mean square differences

$$\text{Err}_{r,r+1}(t) = \left(\int_0^L |\mathbf{x}_r(s, t) - \mathbf{x}_{r+1}(s, t)|^2 ds \right)^{1/2}, \quad (r = 0, 1, 2) \quad (134)$$

where the integrals were approximated by the trapezoidal rule.

If the numerical method is of order μ , we would expect

$$\frac{\text{Err}_{r,r+1}(t)}{\text{Err}_{r+1,r+2}(t)} \approx 2^\mu \quad (135)$$

Figure 6 shows $4^r \text{Err}_{r,r+1}$ for $r = 0, 1, 2$, and Figure 7 shows their ratios. These strongly suggests the numerical methods converge with order at least 2.

10 Conclusion

In this paper, we have presented a robust and fast numerical scheme for simulating the dynamic behavior of elastica in three dimensions. We have employed two sets of techniques:

1. We have used cubic splines for the space discretization. This has proven to be a good discretization. We believe that this may be because the cubic spline is a first order approximation for elastica. It has also been computationally efficient because cubic splines can be computed using tridiagonal matrices.
2. For the time discretization, we derived a numerical scheme that preserves the Hamiltonian. The scheme was derived from the Lagrangian formulation of the dynamics, and the resulting scheme seems to be simpler to understand and implement than other Hamiltonian preserving numerical schemes.

In a later work we plan to extend our work to include the effect of torsion and natural curvature. This will require extending our Hamiltonian preserving scheme to allow quartic terms to appear in the Lagrangian.

11 Acknowledgments

We are very grateful to Professor Yuyi Lin of the University of Missouri for bringing this problem to our attention. This research was supported by a grant from the Research Board of the University of Missouri.

References

- [1] Antman, S. S., 2005, *Nonlinear problems in elasticity*, 2nd edition, Springer, New York.
- [2] Asmar, N. H., 2004, *Partial Differential Equations with Fourier Series and Boundary Value Problems*, 2nd Edition, Prentice Hall.
- [3] Bauchau, O.A. and Bottasso, C.L., 1999, "On the Design of Energy Preserving and Decaying Schemes, for Flexible, Nonlinear Multi-Body Systems," *Computer Methods in Applied Mechanics and Engineering*, 169, pp 61-79.
- [4] Burden, R. L., Faires, J. D., 2005, *Numerical methods*, 8th Edition, Thomson Brooks/Cole Publishing Co.
- [5] Cflisch, R. E., and Maddocks, J. H., 1984, "Nonlinear dynamical theory of the elastica," *Proceedings of the Royal Society of Edinburgh*, Vol 99A, pp. 1-23.
- [6] Celledoni, E., Grimm, V., McLachlan, R.I., McLaren, D.I., O'Neale, D., Owren, B. and Quispel, G.R.W., 2012, "Preserving energy resp. dissipation in numerical PDEs using the 'Average Vector Field' method," *Journal of Computational Physics*, Vol. 231, pp. 6770-6789.
- [7] Coleman, B. D., and Dill, E. H., 1992, "Flexure waves in elastic rods," *J. Acoust. Soc. Am.*, Vol. 91, pp. 2663-2673.
- [8] Dichmann, D.J., Maddocks, J. H., and Pego, R. L., 1996, "Hamiltonian Dynamics of an Elastica and the Stability of Solitary Waves," *Arch. Rational Mech. Anal.*, Vol 135, pp. 357-396.

- [9] Dunford, N., Schwartz, J. T., 1963, Linear operators. Part II. Spectral theory. Selfadjoint operators in Hilbert space. John Wiley & Sons, Inc., New York.
- [10] Falk, R.S., Xu, J.-M., 1995, "Convergence of a second-order scheme for the non-linear dynamical equations of elastic rods," *SIAM J. Numer. Anal.*, Vol. 32, No. 4, pp. 1185-1209.
- [11] Futterer, T., Klar, A. and Wegener, R., 2012, "An Energy Conserving Numerical Scheme for the Dynamics of Hyperelastic Rods," *International Journal of Differential Equations*, Volume 2012, Article ID 718308, 15 pages, doi:10.1155/2012/718308.
- [12] Goss, V. G. A., 2003, Snap buckling, writhing and loop formation in twisted rods, Ph.D. thesis, University College London, <http://myweb.lsbu.ac.uk/~goss/vga/thesisFinal.pdf>.
- [13] Hairer, E. and Wanner, G., 2002, *Solving Ordinary Differential Equations II: Stiff and Differential-Algebraic Problems*, Springer Series in Computational Mathematics, 2nd edition.
- [14] Hall, C.A. and Meyer, W.W., 1976, "Bounds for Cubic Spline Interpolation," *J. Approximation Theory*, Vol 16, pp. 105-122.
- [15] Ito, K., 1998, "Uniform Stabilization of the Dynamic Elastica by Boundary Feedback," *SIAM J. Control Optim.*, Vol. 37, pp. 319-329.
- [16] Ito, K., 2009, "Stabilization of the dynamic elastica only by damping torque," *Nonlinear Analysis: Real World Applications*, Vol. 10, Issue 5, pp. 3122-3131.
- [17] Leimkuhler, B., Reich, S., 2004, *Simulating Hamiltonian Dynamics*, Cambridge University Press, Cambridge.
- [18] Levian, R., 2008, "The Elastica: A Mathematical History," University of California, Berkeley, Technical Report No. UCB/EECS-2008-103, <http://www.eecs.berkeley.edu/Pubs/TechRpts/2008/EECS-2008-103.pdf>.
- [19] Lin, Y., Pisano, A. P., 1987, "General Dynamic Equations of Helical Springs With Static Solution and Experimental Verification," *Transactions of the ASME*, Vol. 54, pp. 910-917.
- [20] Love, A. E. H., 1927, *A Treatise on the Mathematical Theory of Elasticity*, 4th Ed., Dover, New York.
- [21] Maddocks, J. H., and Dichmann, D. J., 1994, "Conservation laws in the dynamics of rods," *Journal of Elasticity*, Vol. 34, pp. 83-96.
- [22] Montgomery-Smith, S.J., and Huang, W., 2012, "Dynamic Equations of Non-Helical Springs," in preparation.
- [23] Pace, B., Diele, F., and Marangi, C., 2012, "Energy Preservation in Separable Hamiltonian Systems by Splitting Schemes," *AIP Conference Proceedings* Volume: 1479 Pages: 1204-1207.
- [24] Pai, F. P., 2007, *Highly Flexible Structures: Modeling, Computation, and Experimentation*, AIAA, Reston, VA.
- [25] Pai, F. P., web page <http://web.missouri.edu/~paip>.
- [26] Preston, S.C., 2011, "The geometry of whips," <http://arxiv.org/abs/1105.1754>.
- [27] Preston, S.C., 2011, "The motion of whips and chains," *Journal of Differential Equations*, Volume 251, Issue 3, August 2011, Pages 504-550.
- [28] Sanz-Serna, J.M. and Calvo, M.P., 1994, *Numerical Hamiltonian problems*, Chapman & Hall.
- [29] Simo, J.C., Marsden, J.E., and Krishnaprasad, P.S., 1988, "The Hamiltonian structure of nonlinear elasticity: The material and convective representations of solids, rods, and plates," *Archive for Rational Mechanics and Analysis*, Volume 104, Number 2, 125-183, DOI: 10.1007/BF00251673.
- [30] Simo, J.C., Wong K.K, 1991, "Unconditionally stable algorithms for rigid body dynamics that exactly preserve energy and momentum," *International Journal for Numerical Methods in Engineering*, Volume 31, Issue 1, pages 19-52, January 1991.
- [31] Simo, J.C. and Tarnow, N., 1992, "The discrete energy-momentum method. Conserving algorithms for nonlinear elastodynamics," *Zeitschrift für Angewandte Mathematik und Physik (ZAMP)*, Volume 43, Number 5, 757-792, DOI: 10.1007/BF00913408.
- [32] Simo, J.C., Tarnow, N., Wong K.K, 1992, "Exact energy-momentum conserving algorithms and symplectic schemes for nonlinear dynamics," *Computer Methods in Applied Mechanics and Engineering*, Volume 100, Issue 1, Pages 63-116.
- [33] Simo, J.C., Tarnow, N. and Doblare, M., 1995, "Non-linear dynamics of three-dimensional rods: Exact energy and momentum conserving algorithms," *International Journal for Numerical Methods in Engineering*, Volume 38, Issue 9, pages 1431-1473.
- [34] Thess, A., Zikanov, O., and Nepomnyashchy A., 1999, "Finite-time singularity in the vortex dynamics of a string," *Physical Review E*, Vol. 59, pp. 3637-3640.
- [35] Thomson, J., 1848, "On the Elasticity and Strength of Spiral Springs," *Cambridge Philosophical and Mathematical Journal*, Vol. 3, pp. 258-266.
- [36] van der Heijden, G. H. M., web page <http://www.ucl.ac.uk/~ucesgvd>.